Article:

Wu, H., Shen, Q., Cui, W. et al. (2021) DOA estimation with nonuniform moving sampling scheme based on a moving platform. IEEE Signal Processing Letters, 28. pp. 1714-1718. ISSN: 1070-9908

https://doi.org/10.1109/lsp.2021.3105035

DOA Estimation with Nonuniform Moving Sampling Scheme Based on a Moving Platform

Hantian Wu, Qing Shen, Wei Cui, Wei Liu, *Senior Member, IEEE*

***Abstract*—The generalized linear moving sampling scheme (MSS) exploiting the second-order statistics and also the high-order cumulants is studied, where the set of MSS is defined as the shifted distance offsets involved in estimation based on a moving platform. Then, sparse physical arrays (SPAs) with nonuniform linear moving sampling schemes (NL-MSS), referred to as SPA-NL-MSS, are proposed to optimize the consecutive difference co-arrays. For the same number of sensors and data samples, better performance in terms of both the number of degrees of freedom (DOFs) and estimation accuracy can be achieved by SPA-NL-MSS than existing array structures exploiting array motions at the second order level.**

***Index Terms*—moving platform, sparse array, difference co-array, DOA estimation, nonuniform moving sampling scheme.**

I. Introduction

Direction of arrival (DOA) estimation based on sparse arrays exploiting the co-array concept has attracted significant interest in the past years [1], [2]. Various specifically designed sparse array structures have been proposed for underdetermined DOA estimation, where nested arrays (NAs) [3], co-prime arrays [4], [5], CACIS and CADiS [6], super nested arrays [7], [8], and thinned co-prime arrays [9] are representative examples based on the second-order difference co-array concept. For the high-order difference co-arrays, multiple level nested arrays [10], simplified and enhanced multiple level nested arrays [11], and other fourth-order cumulant based extensions [12]–[15] have been proposed with improved estimation performance. Furthermore, the difference co-array concept in the spatio-spectral domain was studied in [16]–[19] with significantly increased number of degrees of freedom (DOFs) provided.

All the aforementioned co-arrays are generated from physical arrays on a relatively static platform. Recently, the synthetic aperture was introduced to produce a hole-free difference co-array aided by array motions [20]–[22]. In [23], a dilated nested array (DNA) is designed by increasing the inter-element spacing of an original NA, and the number of DOFs of DNA is three times higher than that of NA with merely one shifted array after motion synthesized at unit spacing $d_0 \leq \frac{\lambda}{2}$ (λ is the signal wavelength) along the end-fire direction of the linear array. This idea is further extended to arbitrary sparse array structures [24], [25], with larger virtual ULA segment in the difference co-array achieved. In [26], a novel approach to construct virtual array exploiting array motion is proposed, tripling the number of DOFs without changing inter-element spacings. Then, in [27], multi-level dilated nested array (ML-DNA) is proposed, where multiple array motions are considered instead of only one fixed motion, leading to increased number of DOFs. However, uniformly shifted arrays after motions are synthesized, and only the second-order difference co-arrays are considered.

In this paper, a series of non-uniform moving sampling schemes with corresponding sparse array construction methods are proposed from the $2q$-th order difference co-array perspective, which also cover the commonly used second-order difference co-array scenario. By grouping each sensor with its shifted versions sampled after moving several specific distances, we find that the $2q$-th ($q \geq 1$) order difference co-array of the synthetic array consists of difference co-arrays of both the physical array and the moving sampled positions, which is then defined as the moving sampling scheme (MSS). The relationship between the physical array and the MSS is studied, and the design of the physical array (spatial sampling scheme) with associated MSS is then proposed to optimize the co-arrays under the criterion of large consecutive co-arrays, forming sparse physical arrays with a nonuniform linear moving sampling scheme. Utilizing both spatial and sparse moving sampling schemes, a better performance in terms of estimation accuracy and the number of DOFs can be achieved for the same number of sensors and data samples.

II. Signal Model Based on a Moving Platform

Consider an N-sensor linear array moving along the array axis at a constant speed v. Denote $\mathbb{S}(t)$ as the position set of moving sensors at time t, expressed as

$$\mathbb{S}(t) = \left\{\hbar_1 d + vt, \hbar_2 d + vt, \hbar_3 d + vt, \ldots, \hbar_N d + vt\right\} , \quad (1)$$

where d is the unit spacing, and $\hbar_n d$, $n = 1, 2, \ldots, N$, is the initial position of the n-th sensor.

Denote $s_k(t)$, $k = 1, 2, \ldots, K$, as the k-th source signal received from angle θ_k, and those source signals are far-field, narrowband, and mutually uncorrelated. Then, the observed signal vector $\mathbf{x}(t)$ is

$$\mathbf{x}(t) = \sum\nolimits_{k=1}^{K} s_k(t) e^{-j\frac{2\pi vt \sin\theta_k}{\lambda}} \mathbf{a}(\theta_k) + \bar{\mathbf{n}}(t) , \quad (2)$$

where $\bar{\mathbf{n}}(t)$ is the $N \times 1$ white Gaussian noise vector, $\mathbf{a}(\theta_k)$ is the steering vector for the original array $\mathbb{S}(0)$ corresponding

This work was supported in part by the National Natural Science Foundation of China under Grants 61801028 and 61628101. (Corresponding author: Qing Shen.)

H. Wu, Q. Shen, and W. Cui are with the School of Information and Electronics, Beijing Institute of Technology, Beijing, 100081, China (e-mails: wuhantian97@163.com, qing-shen@outlook.com, cuiwei@bit.edu.cn)

W. Liu is with the Department of Electronic and Electrical Engineering, University of Sheffield, Sheffield, S1 3JD, UK (e-mail: w.liu@sheffield.ac.uk).

to the k-th source, given as

$$\mathbf{a}(\theta_k) = \left[e^{-j\frac{2\pi\hbar_1 d\sin(\theta_k)}{\lambda}}, \ldots, e^{-j\frac{2\pi\hbar_N d\sin(\theta_k)}{\lambda}}\right]^T . \quad (3)$$

Denote

$$\begin{aligned} \mathbf{A} &= \left[\mathbf{a}(\theta_1), \mathbf{a}(\theta_2), \ldots, \mathbf{a}(\theta_K)\right] \in \mathbb{C}^{N\times K} , \\ \mathbf{s}(t) &= \left[s_1(t)e^{-j\frac{2\pi vt\sin\theta_1}{\lambda}}, \ldots, s_K(t)e^{-j\frac{2\pi vt\sin\theta_K}{\lambda}}\right]^T . \end{aligned} \quad (4)$$

Then, (2) turns into $\mathbf{x}(t) = \mathbf{A}\mathbf{s}(t) + \bar{\mathbf{n}}(t)$. At time $(t+\tau)$, the received signal vector after motion is

$$\begin{aligned} \mathbf{x}(t+\tau) &= \sum\nolimits_{k=1}^{K} s_k(t+\tau)e^{-j\frac{2\pi v(t+\tau)\sin\theta_k}{\lambda}}\mathbf{a}(\theta_k) + \bar{\mathbf{n}}(t+\tau) \\ &= \hat{\mathbf{A}}\mathbf{s}(t+\tau) + \bar{\mathbf{n}}(t+\tau) , \end{aligned} \quad (5)$$

where $\hat{\mathbf{A}} = \left[e^{-j\frac{2\pi v\tau\sin\theta_1}{\lambda}}\mathbf{a}(\theta_1), \ldots, e^{-j\frac{2\pi v\tau\sin\theta_K}{\lambda}}\mathbf{a}(\theta_K)\right]$, and for narrowband signals, assuming τ is small enough so that $s_k(t+\tau) \approx s_k(t)e^{j2\pi f\tau}$ with f being carrier frequency.

Then, (5) is rewritten as $\mathbf{x}(t+\tau) = e^{j2\pi f\tau}\hat{\mathbf{A}}\mathbf{s}(t) + \bar{\mathbf{n}}(t+\tau)$, which can be further translated to

$$\hat{\mathbf{x}}(t+\tau) = e^{-j2\pi f\tau}\mathbf{x}(t+\tau) = \hat{\mathbf{A}}\mathbf{s}(t) + \hat{\mathbf{n}}(t+\tau) , \quad (6)$$

where $\hat{\mathbf{n}}(t+\tau) = e^{-j2\pi f\tau}\bar{\mathbf{n}}(t+\tau)$ after phase compensation.

For this platform, the following assumptions are introduced:

- **A1** The constant moving speed is exactly known in advance.
- **A2** The sources are still far-field compared to the extended aperture, and thus the DOAs of the sources remain the same after motion.
- **A3** The motion time τ should not exceed the signal coherence time [26].

By defining $\tau = \frac{d}{v}$ [23], from (2) and (6) we simply have

$$\mathbf{y}(t) = \begin{bmatrix}\mathbf{x}(t) \\ \hat{\mathbf{x}}(t+\tau)\end{bmatrix} = \begin{bmatrix}\mathbf{A} \\ \hat{\mathbf{A}}\end{bmatrix}\mathbf{s}(t) + \begin{bmatrix}\bar{\mathbf{n}}(t) \\ \hat{\mathbf{n}}(t+\tau)\end{bmatrix} , \quad (7)$$

where the equivalent steering matrix is $\tilde{\mathbf{A}} = [\mathbf{A}^T, \hat{\mathbf{A}}^T]^T$.

Then, existing DOA estimation methods [3], [6], [24], [28] can be applied directly to (7), leading to improved performance due to the extended synthetic virtual array after motion. For the wideband case, group sparsity based methods [18], [29], [30] can be employed, while reduced complexity can be achieved by introducing focusing for pre-processing, followed by either the subspace methods or the CS-based methods [31]–[33].

III. Nonuniform Moving Sampling Scheme

In this section, we first present a generalized moving sampling scheme, and its generated co-arrays are analyzed from both the second-order statistics and higher-order cumulants perspective. Then, the nonuniform moving sampling scheme is proposed with increased DOFs achieved, which is utilized for underdetermined DOA estimation.

A. Generalized Moving Sampling Scheme

Consider the moved array sampled at time $t + \frac{Q_m d}{v}$ as a new one indexed by m, where $\{Q_m\}_{m=1}^{M}$ are unequal positive integers. The sparse array at time t is referred to as the original array. The received signal observed from the m-th moved array at time $(t + \frac{Q_m d}{v})$ is equivalent to that observed from the original array shifted by $Q_m d$ along the direction of motion. For stationary sources, we can obtain a synthetic array composed of the original array and its M shifted arrays.

By stacking all the M shifted arrays, the observed signal vector of the synthetic array can be expressed as

$$\begin{aligned} \mathbf{y}(t) &= \begin{bmatrix}\mathbf{x}(t) \\ \hat{\mathbf{x}}(t+\frac{Q_1 d}{v}) \\ \vdots \\ \hat{\mathbf{x}}(t+\frac{Q_M d}{v})\end{bmatrix} = \begin{bmatrix}\mathbf{A}\mathbf{s}(t) + \bar{\mathbf{n}}(t) \\ \mathbf{A}_1\mathbf{s}(t) + \hat{\mathbf{n}}(t+\frac{Q_1 d}{v}) \\ \vdots \\ \mathbf{A}_M\mathbf{s}(t) + \hat{\mathbf{n}}(t+\frac{Q_M d}{v})\end{bmatrix} \\ &= \tilde{\mathbf{A}}\mathbf{s}(t) + \tilde{\mathbf{n}}(t) , \end{aligned} \quad (8)$$

where $\tilde{\mathbf{A}} = \left[\mathbf{A}^T, \mathbf{A}_1^T \cdots, \mathbf{A}_M^T\right]^T$ and $\tilde{\mathbf{n}}(t) = \left[\bar{\mathbf{n}}(t), \hat{\mathbf{n}}(t+\frac{Q_1 d}{v}), \cdots, \hat{\mathbf{n}}(t+\frac{Q_M d}{v})\right]^T$. The steering matrix of the m-th array is $\mathbf{A}_m = \left[\mathbf{a}_m(\theta_1), \mathbf{a}_m(\theta_2), \ldots, \mathbf{a}_m(\theta_K)\right]$, with

$$\mathbf{a}_m(\theta_k) = \left[e^{-j\frac{2\pi(\hbar_1+Q_m)d\sin(\theta_k)}{\lambda}}, \ldots, e^{-j\frac{2\pi(\hbar_N+Q_m)d\sin(\theta_k)}{\lambda}}\right]^T .$$

According to [24], the sensor positions of the synthetic array can be expressed as

$$\mathbb{S}_{\text{sa}} = \mathbb{S}_0 \cup \mathbb{S}_1 \cup \cdots \cup \mathbb{S}_M , \quad (9)$$

where $\mathbb{S}_0 = \left\{\hbar_1 d, \hbar_2 d, \hbar_3 d, \ldots, \hbar_N d\right\}$ represents the sensor position set of the original array, while the m-th shifted array having sensors located at $\mathbb{S}_m = \mathbb{S}_0 + Q_m d$, where $Q_0 = 0$.

Dividing the sensors in the synthetic array into N groups, each group consists of a physical sensor and its M shifted versions, and (9) is updated to

$$\mathbb{S}_{\text{sa}} = \mathbb{S}_{a1} \cup \mathbb{S}_{a2} \cup \cdots \cup \mathbb{S}_{aN}, \quad (10)$$

where for $n \in \{1, 2, \cdots, N\}$,

$$\mathbb{S}_{an} = \{\hbar_n d + Q_0 d, \hbar_n d + Q_1 d, \cdots, \hbar_n d + Q_M d\} . \quad (11)$$

It is noted that each group $\mathbb{S}_{an_1}$ can be obtained by shifting another group $\mathbb{S}_{an_2}$, i.e., $\mathbb{S}_{an_1} = \mathbb{S}_{an_2} + (\hbar_{n_1}d - \hbar_{n_2}d)$ with $n_1, n_2 \in \{1, 2, \cdots, N\}$. As will be illustrated later, this grouping method is convenient for designing a suitable sparse array configuration based on a moving platform with increased DOFs.

B. Difference Co-Array Analysis from the High-Order Cumulants Perspective

We then derive the $2q$-th order difference co-array of the synthetic array based on the divided groups. The $2q$-th order difference co-array lags of each group is

$$\Phi_{2q} = \left\{ \sum\nolimits_{k=1}^{q} Q_{m_k} - \sum\nolimits_{k=q+1}^{2q} Q_{m_k} \mid 0 \le m_k \le M \right\} .$$

Then, the $2q$-th order difference co-array lags of the synthetic array is obtained by

$$\Phi_{2q_{\text{cp}}} = \cup_{n_1=1}^{N} \cdots \cup_{n_{2q}=1}^{N} \Phi_{2q_{n_1 n_2 \ldots n_{2q}}} , \quad (12)$$

where $\Phi_{2q_{n_1 n_2 \ldots n_{2q}}}$ is the set of difference co-array lags among sensors in $\{\mathbb{S}_{an_k}\}_{k=1}^{2q}$. For $0 \le m_k \le M$,

$$\begin{aligned} \Phi_{2q_{n_1 n_2 \ldots n_{2q}}} &= \sum\nolimits_{k=1}^{q}(Q_{m_k} + \hbar_{n_k}) - \sum\nolimits_{k=q+1}^{2q}(Q_{m_k} + \hbar_{n_k}) \\ &= \Phi_{2q} + \sum\nolimits_{k=1}^{q}\hbar_{n_k} - \sum\nolimits_{k=q+1}^{2q}\hbar_{n_k} . \end{aligned} \quad (13)$$

Note that the $2q$-th order difference co-array lag set of the original array is $\Psi_{2q} = \left\{ \sum_{k=1}^{q} \hbar_{n_k} - \sum_{k=q+1}^{2q} \hbar_{n_k} \mid n_1, n_2, \cdots, n_{2q} = 1, 2 \cdots, N \right\}$, and thus $\Phi_{2q_{\text{cp}}}$ is updated to

$$\Phi_{2q_{\text{cp}}} = \Psi_{2q} + \Phi_{2q}. \tag{14}$$

Eq. (14) indicate that the difference co-array of the synthetic array consists of the difference co-array of both the physical array and the moving sampled positions, and the motion of the array platform leads to increased number of co-arrays. Note that $q = 1$ is a special case which is commonly used in sparse array design and underdetermined DOA estimation, and (14) also works for $q = 1$.

C. Nonuniform Moving Sampling Scheme

The generalized difference co-array set $\Phi_{2q_{\text{cp}}}$ in (14) (which also covers the case exploiting the second-order co-arrays for $q = 1$) depends on the array geometry and the moving sampling positions. The relationship between Φ_{2q} and Ψ_{2q} is important for increasing DOFs, based on which a series of novel sparse array configurations can be designed to reduce co-array redundancies and maximize the virtual ULA segment which is associated with the uniform DOFs (uDOFs).

Remark 1: A large number of consecutive co-array lags is preferred since this virtual ULA segment can be fully exploited by both the co-array MUSIC [34], [35] and the CS-based methods [11], [29]. Therefore, the achievable number of consecutive virtual ULA sensors (also equal to the number of uDOFs) is considered for quantitative evaluation, comparison, and optimal design [6], [11].

Definition 1: The set indicating the moving sampling scheme (MSS) is defined as the set of all shifted offsets involved in estimation, given by

$$\mathbb{S}_{\text{ss}} = \{Q_m d \mid m = 0, 1, \ldots, M\}, \tag{15}$$

where $Q_0 = 0$, and $\{\mathbb{S}_{an}\}_{n=1}^{N}$ in (11) can be expressed as $\mathbb{S}_{an} = \mathbb{S}_{\text{ss}} + \hbar_n d$. The $2q$-th order difference co-array lag set of $\mathbb{S}_{\text{ss}}$ is Φ_{2q}, which is equal to that of $\{\mathbb{S}_{an}\}_{n=1}^{N}$.

Then, the structure construction problem with increased uDOFs is translated to the design of both the moving sampling scheme $\mathbb{S}_{\text{ss}}$ and the physical array configuration $\mathbb{S}_0$.

For an arbitrary array geometry, we assume that the maximum number of consecutive co-array lags in Φ_{2q} and Ψ_{2q} are $N_{\Phi,2q}$ and $N_{\Psi,2q}$, respectively. Denote $d_0 \leq \frac{\lambda}{2}$ as a reference spacing. The unit spacing of the physical array is $d = P_{\text{pa}} d_0$, while the unit moving sampling spacing (the minimum sampling spacing) is $d_{\text{ss}} = P_{\text{ss}} d_0$.

Proposition 1: For $P_{\text{pa}} = N_{\Phi,2q}$ and $P_{\text{ss}} = 1$, the maximum number of uDOFs of the synthetic array can be achieved, which is $N_{\text{sa}} = N_{\Phi,2q} \cdot N_{\Psi,2q}$. The conclusion also fits the case where $P_{\text{pa}} = 1$ and $P_{\text{ss}} = N_{\Psi,2q}$.

Proof: We focus on the case of $P_{\text{pa}} = N_{\Phi,2q}$ and $P_{\text{ss}} = 1$ hereafter, and the proof for $P_{\text{pa}} = 1$ and $P_{\text{ss}} = N_{\Psi,2q}$ is similar.

The number of consecutive co-arrays of the MSS set $\mathbb{S}_{\text{ss}}$ is assumed to be $N_{\Phi,2q}$. As a result, for every virtual uniform linear co-array $\beta_j d$ $(j = 1, 2, \ldots, N_{\Psi,2q})$ in $\Psi_{2q} d$, the associated consecutive co-array set introduced by the addition operation in (14) is

$$\phi_{\beta_j} = \left\{ \gamma_j \mid \beta_j - \tfrac{N_{\Phi,2q}-1}{2} \leq \gamma_j \leq \beta_j + \tfrac{N_{\Phi,2q}-1}{2} \right\}. \tag{16}$$

Note that $N_{\Phi,2q}$ is odd since the co-arrays are symmetric about zero. When $P_{\text{pa}} = N_{\Phi,2q}$ with $\beta_{j+1} - \beta_j = N_{\Phi,2q}$, it is obvious that the sets ϕ_{β_j} $(j = 1, 2, \ldots, N_{\Psi,2q})$ are non-overlapped and adjacent to each other, leading to the largest number of uDOFs provided by the synthetic array, i.e., $N_{\text{sa}} = N_{\Phi,2q} \cdot N_{\Psi,2q}$. The addition operation in (14) fills the holes between adjacent co-arrays in $\Psi_{2q} d$. ∎

Definitely, more spatial sampling points in the scheme, i.e., a larger M, leads to significantly increased consumption of resources and complexity, including data storage and computations. When the uniform linear moving sampling scheme (UL-MSS) is applied with $Q_m = m$, $m = 0, 1, \ldots, M$, we have $N_{\Psi,2q} = 2qM + 1$ and thus $N_{\text{sa}} = N_{\Phi,2q} \cdot (2qM + 1)$. On the contrary, for a fixed M without introducing extra complexity, more DOFs can be provided using the nonuniform (sparse) linear moving sampling scheme (NL-MSS).

Similarly, for a fixed N, the number of DOFs can be further increased by employing a nonuniform physical array with a unit spacing $d = N_{\Psi,2q} d_0$ according to *Proposition 1*.

Remark 2: The proposed array structure is referred to as a sparse physical array with nonuniform linear moving sampling scheme (SPA-NL-MSS). Generally, arbitrary sparse arrays can be employed as the physical array and the moving sampling scheme. Therefore, $O\big((M+1)^{2q} N^{2q}\big)$ DOFs can be provided by a specifically designed SPA-NL-MSS.

The multi-level nested array (MLNA) [10] is taken as an MSS example. Denote $M_0 = 1$, and set $M + 1 = \sum_{i=1}^{2q} (M_i - 1) + 1$ sensors, which are located in the n-th group $\mathbb{S}_{an} = \cup_{i=1}^{2q} \mathbb{S}_{an,i}$, where the i-th sub-array $\{\mathbb{S}_{an,i}\}_{i=1}^{2q-1}$ of $\mathbb{S}_{an}$ holds $M_i - 1$ sensors in

$$\mathbb{S}_{an,i} = \left\{ \left(\hbar_n + m \prod_{j=0}^{i-1} M_j - 1 \right) d_{\text{ss}}, m = 1, \ldots, M_i - 1 \right\},$$

while the $2q$-th sub-array has M_{2q} sensors located at

$$\mathbb{S}_{an,2q} = \left\{ \left(\hbar_n + m \prod_{j=0}^{2q-1} M_j - 1 \right) d_{\text{ss}}, m = 1, \ldots, M_{2q} \right\}.$$

The maximum number of consecutive co-arrays of the $2q$-level nested moving sampling scheme ($2q$LN-MSS) is $N_{\Phi,2q}$, given by

$$N_{\Phi,2q} = \begin{cases} 2M_1 M_2 - 1, & q = 1, \\ 2\left(\prod_{j=1}^{2q} M_j + \prod_{j=1}^{2q-1} M_j \right) - 1, & q \geq 2. \end{cases} \tag{17}$$

Considering $d_{\text{ss}} = d_0$ and a $2q$-level nested array with its unit spacing being $d = N_{\Phi,2q} d_0$, a $2q$-level nested array with $2q$LN-MSS ($2q$LNA-$2q$LN-MSS) is formed. The number of physical sensors in the $2q$LNA is $N = \sum_{i=1}^{2q} (N_i - 1) + 1$, where $\{N_i - 1\}_{i=1}^{2q-1}$ is the sensor number of the i-th subarray, while N_{2q} is that of the $2q$-th subarray.

The number of uDOFs provided by $2q$LNA-$2q$LN-MSS is

$$N_{\text{sa}} = \begin{cases} (2N_1 N_2 - 1)(2M_1 M_2 - 1), & q = 1, \\ \left(2\left(\prod_{j=1}^{2q} N_j + \prod_{j=1}^{2q-1} N_j \right) - 1 \right) & \\ \times \left(2\left(\prod_{j=1}^{2q} M_j + \prod_{j=1}^{2q-1} M_j \right) - 1 \right), & q \geq 2. \end{cases} \tag{18}$$

TABLE I
COMPARISON OF THE NUMBER OF UDOFS AMONG DIFFERENT STRUCTURES WITH VARIOUS NUMBER OF SENSORS

Sensor Number N / Structures, $\mathbb{S}_{ss}$, M	4(3,2) (2,2,2,1)	6(4,3) (3,2,2,2)	8(5,4) (3,3,3,2)
NA[1] ($q=1$)	11	23	39
DNA[2], $\{0,1\}d$, $M=1$	33	69	117
ML-DNA[3], $\{0,1,2\}d$, $M=2$	55	115	195
2LNA-2LN-MSS[4], $\{0,1,3\}d$, $M=2$	77	161	273
2LNA-2LN-MSS, $\{0,1,2,5,8\}d$, $M=4$	187	391	663
4LNA[5] ($q=2$)	29	71	161
4LNA-4LN-MSS[6], $\{0,1,3,7,15\}d$, $M=4$	1363	3337	7567

[1]NA: Nested Array [3]. [2]DNA: Dilated Nested Array [23].
[3]ML-DNA: Multi-Level Dilated Nested Array [27].
[4]2LNA-2LN-MSS: Two Level NA with Two Level Nested MSS.
[5]4LNA: Four Level Nested Array [10].
[6]4LNA-4LN-MSS: Four Level NA with Four Level Nested MSS.

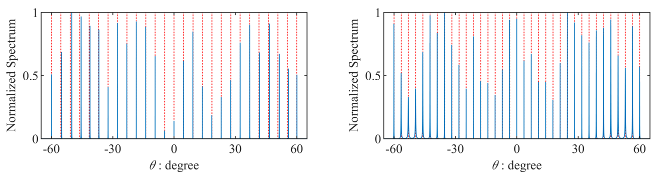

(a) ML-DNA, $K=27$ (b) 2LNA-2LN-MSS, $K=35$

Fig. 1. DOA estimation results of different array structures.

IV. SIMULATION RESULTS

We first compare the number of uDOFs for arrays with different moving sampling schemes. Multi-level dilated nested array (ML-DNA) [27] and dilated nested array (DNA) [23] are nested arrays with uniform linear MSS for $M \geq 2$ and $M=1$, respectively. The maximum number of consecutive difference co-arrays of NA, DNA, ML-DNA, 2LNA-2LN-MSS exploiting the second-order statistics ($q=1$) and 4LNA, 4LNA-4LN-MSS based on the fourth-order statistics ($q=2$) are listed in Table I, where optimal array structures offering the highest uDOFs among potential configurations are employed [10], referred to as (N_1, N_2) for $q=1$ and (N_1, N_2, N_3, N_4) for $q=2$ as indicated in Table I. Clearly, the proposed $2q$LNA-$2q$LN-MSS provides a higher number of uDOFs than the other structures with the same sensor number N. Furthermore, with the same number of moving sampling steps M, i.e., the same data samples in total, the number of uDOFs increases with q significantly for a fixed N by employing the NL-MSS.

Then we evaluate the DOA estimation performance, where the K uncorrelated far-field sources are uniformly distributed between $-60°$ and $60°$, and the SS-MUSIC method is employed. The maximum number of sources that can be resolved is $\frac{N_{sa}-1}{2}$. As shown in Table I, up to 27 and 38 sources can be resolved for $N=4$ using ML-DNA and 2LNA-2LN-MSS respectively. Fig.1 gives the DOA estimation results obtained by ML-DNA when $K=27$ and NA-NL-MSS when $K=35$, where the input SNR is fixed to 0dB with 10000 snapshots. Note that SS-MUSIC based on ML-DNA fails to resolve 28 sources since the MUSIC spectrum cannot be obtained for $K \geq \frac{N_{sa}-1}{2}$. More sources can be resolved by the proposed 2LNA-2LN-MSS.

Finally, the root mean square error (RMSE) results are examined. The nested array with $N=6$ and $(N_1, N_2)=(4,3)$ is employed, while the unit spacings d for NA, DNA, ML-DNA, and 2LNA-2LN-MSS with $\mathbb{S}_{ss}=\{0,1,3\}$ are d_0, $3d_0$, $5d_0$, and $7d_0$, respectively, where $d_0=\frac{\lambda}{2}$. The RMSE results versus the input SNR and the number of snapshots are shown in Fig. 2(a) (500 snapshots) and Fig. 2(b) (0dB SNR), respectively. Clearly, the performance of the proposed 2LNA-2LN-MSS is better than other existing structures due to the increased uDOFs.

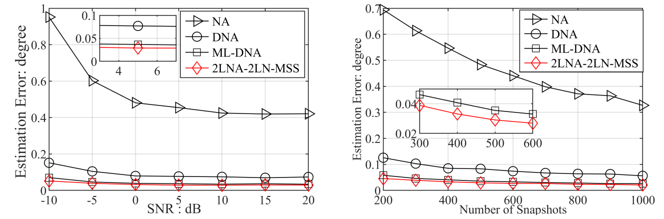

(a) RMSE results versus SNR ($q=1$)(b) RMSE results versus the number of snapshots ($q=1$)

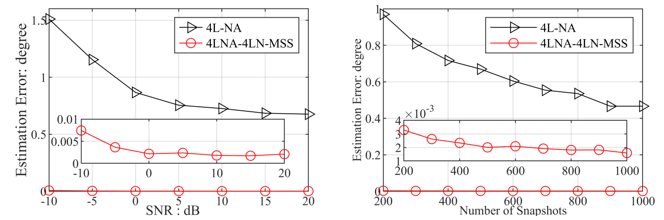

(c) RMSE results versus SNR ($q=2$)(d) RMSE results versus the number of snapshots ($q=2$)

Fig. 2. RMSE results of different array structures.

We then focus on the performance exploiting the fourth order cumulants with $q=2$, and the proposed structure 4LNA-4LN-MSS with $\mathbb{S}_{ss}=\{0,1,3,7,15\}d$ is compared with its parent structure 4LNA with $N=6$ and $(N_1, N_2, N_3, N_4)=(3,2,2,2)$, and their unit spacings are $47d_0$ and d_0, respectively. As shown in Figs. 2(c) and 2(d), It is obvious that by employing the sparse moving sampling scheme, better performance can be achieved by 4LNA-4LN-MSS.

V. CONCLUSION

The underdetermined DOA estimation problem based on a moving platform was studied, and the relationship between the MSS set and the physical array to provide significantly increased DOFs was derived under the criterion of large consecutive co-arrays via exploiting the $2q$-th order cumulants. Utilizing both spatial and moving sparse sampling schemes, sparse physical arrays with nonuniform linear moving sampling scheme (SPAs-NL-MSS) were proposed. It has been shown by simulations that for the same sensor number and data samples, the proposed 2LNA-2LN-MSS with nested scheme ($q=1$) outperforms other existing array structures in terms of estimation accuracy and the number of DOFs, and further improvements can be achieved by increasing q with the specifically designed $2q$ level nested scheme employed.

REFERENCES

[1] R. T. Hoctor and S. A. Kassam, "The unifying role of the coarray in aperture synthesis for coherent and incoherent imaging," *Proc. IEEE*, vol. 78, no. 4, pp. 735–752, Apr. 1990.

[2] Q. Shen, W. Liu, W. Cui, and S. Wu, "Underdetermined DOA estimation under the compressive sensing framework: A review," *IEEE Access*, vol. 4, pp. 8865–8878, 2016.

[3] P. Pal and P. P. Vaidyanathan, "Nested arrays: a novel approach to array processing with enhanced degrees of freedom," *IEEE Trans. Signal Process.*, vol. 58, no. 8, pp. 4167–4181, Aug. 2010.

[4] P. P. Vaidyanathan and P. Pal, "Sparse sensing with co-prime samplers and arrays," *IEEE Trans. Signal Process.*, vol. 59, no. 2, pp. 573–586, Feb. 2011.

[5] P. Pal and P. P. Vaidyanathan, "Coprime sampling and the MUSIC algorithm," in *Proc. IEEE Digital Signal Processing Workshop and IEEE Signal Processing Education Workshop(DSP/SPE)*, Sedona, AZ, Jan. 2011, pp. 289–294.

[6] S. Qin, Y. D. Zhang, and M. G. Amin, "Generalized coprime array configurations for direction-of-arrival estimation," *IEEE Trans. Signal Process.*, vol. 63, no. 6, pp. 1377–1390, March 2015.

[7] C.-L. Liu and P. Vaidyanathan, "Super nested arrays: Linear sparse arrays with reduced mutual coupling-part i: Fundamentals," *IEEE Trans. Signal Process.*, vol. 64, no. 15, pp. 3997–4012, Aug. 2016.

[8] C.-L. Liu and P. P. Vaidyanathan, "Super nested arrays: Linear sparse arrays with reduced mutual coupling-part ii: High-order extensions," *IEEE Trans. Signal Process.*, vol. 64, no. 16, pp. 4203–4217, Aug. 2016.

[9] A. Raza, W. Liu, and Q. Shen, "Thinned coprime array for second-order difference co-array generation with reduced mutual coupling," *IEEE Trans. Signal Process.*, vol. 67, no. 8, pp. 2052–2065, 2019.

[10] P. Pal and P. Vaidyanathan, "Multiple level nested array: An efficient geometry for $2q$th order cumulant based array processing," *IEEE Trans. Signal Process.*, vol. 60, no. 3, pp. 1253–1269, Mar. 2012.

[11] Q. Shen, W. Liu, W. Cui, S. Wu, and P. Pal, "Simplified and enhanced multiple level nested arrays exploiting high-order difference co-arrays," *IEEE Trans. Signal Process.*, vol. 67, no. 13, pp. 3502–3515, Jul. 2019.

[12] Q. Shen, W. Liu, W. Cui, and S. Wu, "Extension of co-prime arrays based on the fourth-order difference co-array concept," *IEEE Signal Process. Lett.*, vol. 23, no. 5, pp. 615–619, May 2016.

[13] A. Ahmed, Y. D. Zhang, and B. Himed, "Effective nested array design for fourth-order cumulant-based doa estimation," in *Proc. IEEE Radar Conference (RadarConf)*, 2017, pp. 0998–1002.

[14] J. Cai, W. Liu, R. Zong, and Q. Shen, "An expanding and shift scheme for constructing fourth-order difference coarrays," *IEEE Signal Process. Lett.*, vol. 24, no. 4, pp. 480–484, Apr. 2017.

[15] Z. Yang, Q. Shen, W. Liu, Y. C. Eldar, and W. Cui, "Extended cantor arrays with hole-free fourth-order difference co-arrays," in *Proc. IEEE International Symposium on Circuits and Systems (ISCAS)*. IEEE, 2021, pp. 1–5.

[16] Q. Shen, W. Liu, W. Cui, S. Wu, Y. D. Zhang, and M. G. Amin, "Wideband DOA estimation for uniform linear arrays based on the co-array concept," in *Proc. European Signal Processing Conference (EUSIPCO)*, Nice, France, Sep. 2015, pp. 2885–2889.

[17] S. Qin, Y. D. Zhang, M. G. Amin, and B. Himed, "DOA estimation exploiting a uniform linear array with multiple co-prime frequencies," *Signal Processing*, vol. 130, pp. 37–46, Jan. 2017.

[18] H. Wu, Q. Shen, W. Liu, and W. Cui, "Underdetermined low-complexity wideband DOA estimation with uniform linear arrays," in *Proc. IEEE Sensor Array and Multichannel Signal Processing Workshop (SAM)*, 2020, pp. 1–5.

[19] Y. Liang, W. Cui, Q. Shen, W. Liu, and H. Wu, "Cramer-rao bound for DOA estimation exploiting multiple frequency pairs," *IEEE Signal Process. Lett.*, vol. 28, pp. 1210–1214, 2021.

[20] J. Ramirez Jr and J. L. Krolik, "Synthetic aperture processing for passive co-prime linear sensor arrays," *Digit. Signal Process.*, vol. 61, pp. 62–75, 2017.

[21] J. Ramirez, J. Odom, and J. Krolik, "Exploiting array motion for augmentation of co-prime arrays," in *Proc. IEEE Sensor Array and Multichannel Signal Processing Workshop (SAM)*, 2014, pp. 525–528.

[22] J. Ramirez and J. Krolik, "Multiple source localization with moving co-prime arrays," in *Proc. IEEE International Conference on Acoustics, Speech and Signal Processing (ICASSP)*, 2015, pp. 2374–2378.

[23] G. Qin, Y. D. Zhang, and M. G. Amin, "DOA estimation exploiting moving dilated nested arrays," *IEEE Signal Process. Lett.*, vol. 26, no. 3, pp. 490–494, 2019.

[24] G. Qin, M. G. Amin, and Y. D. Zhang, "DOA estimation exploiting sparse array motions," *IEEE Trans. Signal Process.*, vol. 67, no. 11, pp. 3013–3027, 2019.

[25] S. Li and X. Zhang, "A novel moving sparse array geometry with increased degrees of freedom," in *Proc. IEEE International Conference on Acoustics, Speech and Signal Processing (ICASSP)*, 2020, pp. 4767–4771.

[26] ——, "A new approach to construct virtual array with increased degrees of freedom for moving sparse arrays," *IEEE Signal Process. Lett.*, vol. 27, pp. 805–809, 2020.

[27] Y. Zhou, Y. Li, and C. Wen, "The multi-level dilated nested array for direction of arrival estimation," *IEEE Access*, vol. 8, pp. 43 134–43 144, 2020.

[28] Y. D. Zhang, M. G. Amin, and B. Himed, "Sparsity-based DOA estimation using co-prime arrays," in *Proc. IEEE International Conference on Acoustics, Speech and Signal Processing (ICASSP)*, Vancouver, Canada, May 2013, pp. 3967–3971.

[29] Q. Shen, W. Liu, W. Cui, S. Wu, Y. D. Zhang, and M. G. Amin, "Low-complexity direction-of-arrival estimation based on wideband co-prime arrays," *IEEE/ACM Trans. Audio, Speech, Language Process.*, vol. 23, no. 9, pp. 1445–1456, Sep. 2015.

[30] Q. Shen, W. Cui, W. Liu, S. Wu, Y. D. Zhang, and M. G. Amin, "Underdetermined wideband DOA estimation of off-grid sources employing the difference co-array concept," *Signal Processing*, vol. 130, pp. 299–304, 2017.

[31] Q. Shen, W. Liu, W. Cui, S. Wu, Y. D. Zhang, and M. G. Amin, "Focused compressive sensing for underdetermined wideband DOA estimation exploiting high-order difference coarrays," *IEEE Signal Process. Lett.*, vol. 24, no. 1, pp. 86–90, Jan. 2017.

[32] W. Cui, Q. Shen, W. Liu, and S. Wu, "Low complexity DOA estimation for wideband off-grid sources based on re-focused compressive sensing with dynamic dictionary," *IEEE J. Sel. Topics Signal Process.*, vol. 13, no. 5, pp. 918–930, 2019.

[33] Q. Shen, W. Liu, L. Wang, and Y. Liu, "Group sparsity based localization for far-field and near-field sources based on distributed sensor array networks," *IEEE Trans. Signal Process.*, vol. 68, pp. 6493–6508, 2020.

[34] C.-L. Liu and P. P. Vaidyanathan, "Remarks on the spatial smoothing step in coarray MUSIC," *IEEE Signal Process. Lett.*, vol. 22, no. 9, pp. 1438–1442, Sep. 2015.

[35] C.-L. Liu and P. P. Vaidyanathan, "Robustness of difference coarrays of sparse arrays to sensor failures-part I: A theory motivated by coarray MUSIC," *IEEE Trans. Signal Process.*, vol. 67, no. 12, pp. 3213–3226, Jun. 2019.